

Modeling of WalkMECH: a Fully-Passive Energy-Efficient Transfemoral Prosthesis Prototype

R. Unal^{*†}, F. Klijstra^{*}, B. Burkink^{*}, S.M. Behrens[†], E.E.G. Hekman[†],
S. Stramigioli^{*}, H.F.J.M. Koopman[†] and R. Carloni^{*}

^{*}Robotics and Mechatronics Engineering Laboratory

[†]Biomechanical Engineering Laboratory

University of Twente, Enschede, The Netherlands

Emails: {r.unal, f.klijstra, b.burkink, s.m.behrens, e.e.g.hekman, s.stramigioli, h.f.j.m.koopman, r.carloni}@utwente.nl

Abstract—In this paper we present the port-based model of WalkMECH, a fully-passive transfemoral prosthesis prototype that has been designed and realized for normal walking. The model has been implemented in a simulation environment so to analyze the performance of the prosthetic leg in walking experiments and so to enhance the mechanics of the system. The accuracy of the model has been validated by experimental tests with a unilateral amputee participant.

I. INTRODUCTION

A transfemoral prosthesis is an assistive device, which artificially replaces the lower limb after an amputation due to a trauma or a disease. The challenging part in designing and realizing such a device is in reducing the use of metabolic energy consumption while restoring the gait pattern of the amputee with a light-weighted and intuitive system. In our previous work, we designed and realized a fully-passive transfemoral prosthesis prototype for normal walking, WalkMECH, which provides 76% of the required energy for the ankle push-off generation [1], [2]. The conceptual design is based on the analysis of the energetics of walking of the natural human gait with the final goal of having an energy efficient device [3], [4]. This is done by including three elastic elements, which realize an energetic coupling between the knee and the ankle joints. More precisely, three elastic elements are engaged in different phases of the stride and they mimic the muscles synergies found in the healthy human gait.

In order to evaluate the performance of the system and optimize the parameters of the design, models for simulations are commonly employed. The creation of a dynamic model to generate gait patterns poses challenges such as the level of complexity and the adaptability to design changes. A model of human body dynamics is shown using a mechanical multi-body system approach in [5]. The same strategy of modeling has been used in [6] and [7]. These models are made with the main purpose of obtaining gait patterns. Detailed analyses and simulations of human gait has been presented in [8], [9], in which the muscle coordinations and the clinical implications have been discussed. A dynamical model of a transfemoral prosthesis derived by using Lagrange method has been presented in [10] as a two-dimensional multi-body dynamic system. These studies show the requirements and advantages of modeling the prosthetic prototypes and they

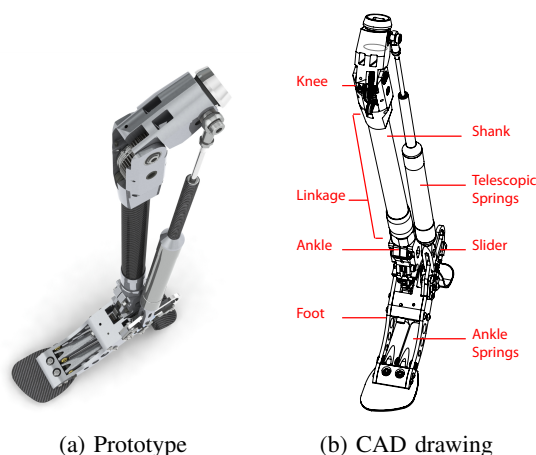


Fig. 1: Mechanical realization of WalkMECH.

highlight the challenges of modeling due to its complex nature.

At the current stage of our research, a detailed dynamic model of the complete system is necessary to investigate how the transfemoral prosthesis prototype is performing in terms of kinematics and kinetics. The model will be used for the analysis of the transfemoral prototype to look for further improvements and eventually realizations. For this reason, we built a port-based model in a simulation environment, which founds its basis on screw theory, and we validated it through experimental tests realized with a unilateral transfemoral amputee participant.

The remainder of the paper is organized as follows. Section II presents the working principle of the transfemoral prosthesis prototype WalkMECH. The complete model is presented in Section III and validated in Section IV through experimental tests. Finally, conclusions are drawn in Section V.

II. WORKING PRINCIPLE OF WALKMECH

The transfemoral prosthesis prototype WalkMECH is shown in Fig. 1, in which both a picture of the realized system and a CAD drawing are depicted. The transfemoral prosthesis is a fully-passive system, which has been designed and realized to mimic the human gait, especially in terms of energetics [2].

Fig. 2 shows the power flow at the knee (top) and ankle (bottom) joints in a healthy human during natural gait [11].

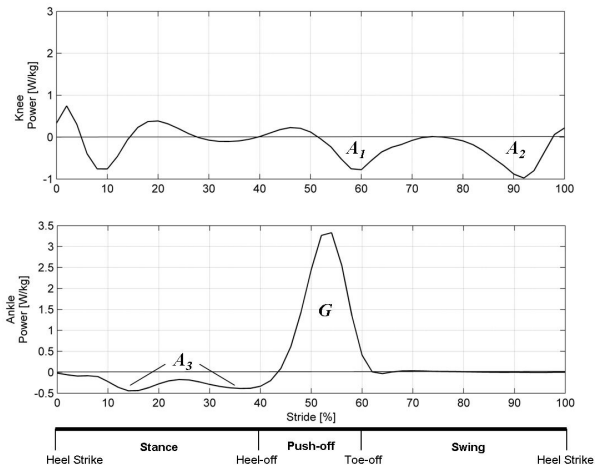


Fig. 2: The power flow of the healthy human gait normalized in body weight in the knee (top) and the ankle (bottom) joints during one stride at normal speed [11]. The areas $A_{1,2,3}$ indicate the energy absorption, whereas G indicates the energy generation. The cycle is divided into three phases (stance, push-off and swing) with three main instants (heel-strike, heel-off and toe-off).

In the figure, it is possible to identify three instants, i.e. heel strike, push-off and toe-off, and three main phases:

- Stance: The knee absorbs a certain amount of energy during its flexion and generates as much as the same amount of energy for its extension. In the meantime, the ankle joint absorbs energy due to the weight bearing, represented by A_3 .
- Push-off: The knee starts absorbing energy, represented by A_1 in the figure, while the ankle generates the main part of the gait energy for the push-off, represented by G , which is about the 80% of the overall generation.
- Swing: The knee absorbs energy, represented by A_2 in the figure, during the late swing phase, while the energy in the ankle joint is negligible.

These energetic phases show that there is almost a complete balance between the generated and the absorbed energy, since the energy for push-off generation (G) is almost the same as the total energy absorbed in the three intervals $A_{1,2,3}$.

In its working principle, the transfemoral prosthesis absorbs energy during stance, swing phase and at heel strike, and it releases energy during ankle push-off. This has been realized by using three storage elements as depicted in Fig. 3 and explained hereafter, i.e.:

- The linkage mechanism C_L couples the knee and ankle joints kinematically and is responsible for the transfer of a part of A_1 to the ankle push-off generation (G), as a consequence of the closed-loop kinematic chain.
- The elastic element C_2 couples the upper and lower leg, and its attachment point can move on the foot. C_2 stores the kinetic energy of the lower leg (A_2) during swing motion. At the beginning of the swing phase, the attachment point of C_2 is changed from the heel to the upper part of the foot. At the end of the swing, the spring

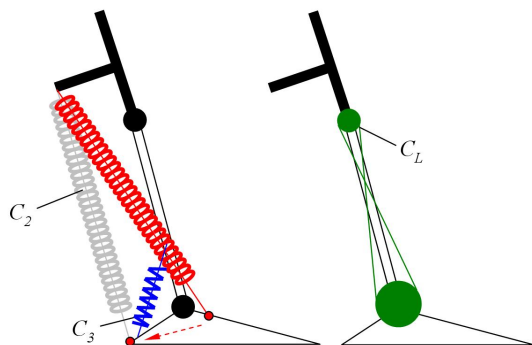


Fig. 3: Conceptual design of the proposed mechanism (given separately for better interpretation) - The design presents three elastic elements: C_2 between the foot and the upper leg, C_3 between the foot and the lower leg (left), a linkage system C_L between the knee and ankle joints (right).

is loaded and its position changes back to the heel for releasing the stored energy for ankle push-off.

- The ankle elastic element C_3 connects the foot and the lower leg and is responsible for the main part of the absorption A_3 . During the stance phase, i.e. while the ankle is in dorsiflexion motion, a braking torque is applied to the ankle in order to bear the weight of the body. Instead of dissipating the energy by using a brake system, this elastic element provides the brake torque and stores the energy A_3 .

III. MODEL

In this Section, we present the model of WalkMECH. First, we give a short overview of the notations and of the mathematical framework and, afterwards, each part of the device is discussed in details.

A. Overall Kinematics

The construction of the dynamic model has been realized in the simulation environment 20-sim (Controllab Products B.V., The Netherlands). More information on the mathematical framework can be found in [12].

A complete overview of all the joints and bodies of the transfemoral prosthesis is shown in Fig. 4. Every joint is described in its coordinate frame. The joints 0, 1, 2, 3, 6, 8 are rotational joints and can rotate freely around their local y direction. The joints 4 and 7 are translational joints and can translate freely along their local z direction, so to realize the coupling elastic element C_2 and the ankle elastic element C_3 . The joint 5 can both translate along its local z direction and can rotate around its local y direction, so to realize the sliding action of the attachment point of C_2 on the foot. All joints are summarized in Table I.

B. Coupling and Ankle Elastic Elements

The location of the coupling elastic element C_2 is in between joint 3 and 4 and it has a progressive behaviour in order to realize the natural knee flexion [1]. In particular, the force exerted by this element depends on the spring state

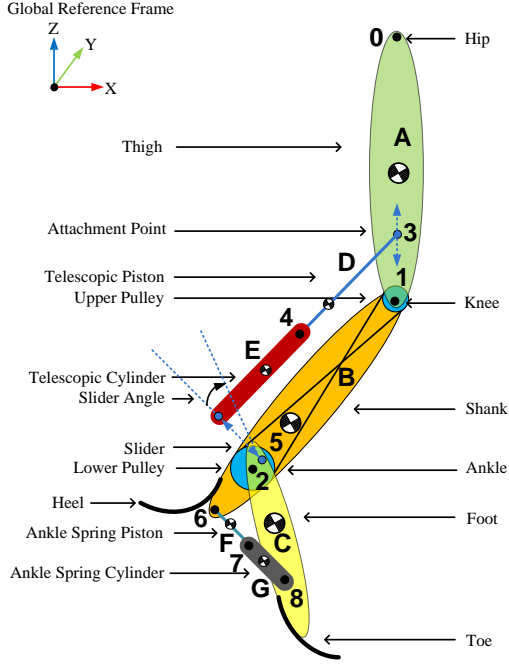


Fig. 4: Schematic overview of WalkMECH, where bodies are represented by letters and joints by numbers.

TABLE I: Joint representation and degrees of freedom (DOFs) with respect to local reference frames.

Joint in the Physical System	Joint Number	Local DOFs
Hip	0	X, Z and Ry
Knee	1	Ry
Ankle	2	Ry
Upper Attachment Point	3	Ry
Coupling Elastic Element	4	Z
Slider	5	Ry and Z
Heel Attachment Point	6	Ry
Ankle Elastic Element	7	Ry
Toe Attachment Point	8	Ry

x and on the elastic constants of the three springs that are progressively engaged, i.e.:

$$F_{C_2} = \begin{cases} k_1 (x - x_0) & 0 < x \leq s_1 \\ (k_1 + k_2) (x - x_0) & s_1 < x \leq s_2 \\ (k_1 + k_2 + k_3) (x - x_0) & x > s_2 \\ k_0 (x - x_0) & x < 0 \end{cases}$$

where x_0 is the zero length of the spring and k_i the elastic constants implemented in WalkMECH.

The ankle elastic element is a linear spring with k_4 as elastic constant. The force exerted by this spring is given by

$$F_{C_3} = k_4 \cdot (x - x_0), \quad x > 0$$

where x_0 is the zero length of the spring.

C. Linkage

The linkage, C_L is located between the knee and ankle joints, as shown in Fig. 4. This element can be modeled as a conditional spring since it is not continuously active. The

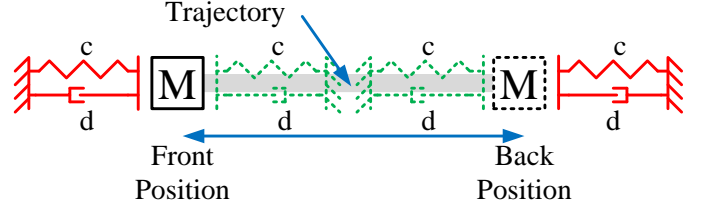


Fig. 5: Slider Schematic.

connection is activated between heel-off and toe-off (around 44% - 60% of the stride) as it is designed on the prototype. Then the connection is disengaged and the ankle and knee are not coupled anymore.

D. Slider

The slider can move freely along the local z direction of the joint 5, as shown in Fig. 4. Schematic representation of the slider is shown in Fig. 5, and the mass represents the telescopic cylinder, i.e. the support of the elastic element C_2 . The following relations hold for the inner and outer bounds for the front and back position of the slider, i.e.,

$$\text{front} = \begin{cases} \text{outer bound} & \text{always valid} \\ \text{inner bound} & \phi_{\text{ankle}} < \phi_{\text{release_ankle}} \end{cases}$$

$$\text{back} = \begin{cases} \text{outer bound} & \text{always valid} \\ \text{inner bound} & \text{coupling is pulling} \end{cases}$$

where $\phi_{\text{release_ankle}}$ is a release angle for the slider that is set with the ankle joint according to the walking speed. The outer bounds represent the front and back-end position of the slider since it can not move any further in the physical system [1]. The inner bound on the back position models the groove at the back that holds the slider.

E. Ground Reaction Forces

The implementation of the ground reaction forces is based on the Hunt-Crossley model for ground interaction [13]. The Hunt-Crossley contact model is used to calculate the normal force which is exerted by the ground and the friction force which acts parallel to the ground. Fig. 6 schematically displays the implementation of the contact model.

In the dynamic simulation of the model, the contact point is calculated as the closed contact from a circle (e.g., the heel profile) with respect to another point (e.g., the ground), to create the necessary roll-over, as explained in [13], i.e.,

$$\mathbf{H}_{heel}^0 = \mathbf{H}_{p_2}^0 \mathbf{H}_{heel}^{p_2} \quad (1)$$

The interaction circle center, H_{icc} with the radius, r , of the circle is given by:

$$\mathbf{H}_{icc}^0 = \mathbf{H}_{heel}^0 \begin{bmatrix} 1 & 0 & 0 & 0 \\ 0 & 1 & 0 & 0 \\ 0 & 0 & 1 & r \\ 0 & 0 & 0 & 1 \end{bmatrix} \quad (2)$$

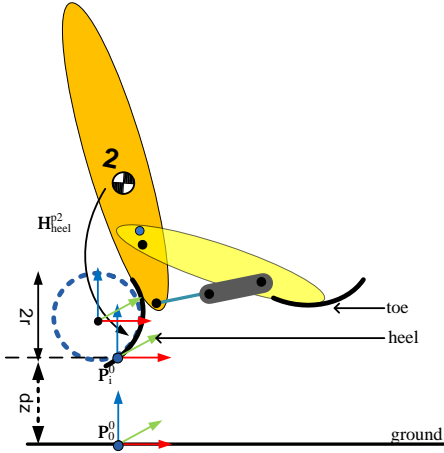


Fig. 6: Schematic overview of ground interaction closest point.

The x and z positions, i.e., \mathbf{z}_0 , from the heel with respect to the ground is given by:

$$\mathbf{z}_0(x_i) = \mathbf{H}_{icc}(1:3,1) \bullet \begin{bmatrix} 0 \\ 0 \\ 1 \end{bmatrix} \quad (3)$$

$$\mathbf{z}_0(z_i) = \mathbf{H}_{icc}(1:3,3) \bullet \begin{bmatrix} 0 \\ 0 \\ 1 \end{bmatrix} \quad (4)$$

The position of the point on the closed circle with respect to the ground is derived by the following equations, where ϵ is a very small number for the calculation purposes,

$$\mathbf{P}_i^i = \begin{bmatrix} \frac{-r \cdot \mathbf{z}_0(x_i)}{\sqrt{\mathbf{z}_0(x_i)^2 + \mathbf{z}_0(z_i)^2 + \epsilon}} \\ 0 \\ \frac{-r \cdot \mathbf{z}_0(z_i)}{\sqrt{\mathbf{z}_0(x_i)^2 + \mathbf{z}_0(z_i)^2 + \epsilon}} \\ 1 \end{bmatrix} \quad (5)$$

$$\mathbf{P}_i^0 = \mathbf{H}_{icc} \mathbf{P}_i^i \quad (6)$$

The interaction point H_{ip} is given by:

$$\mathbf{H}_{ip} = \begin{bmatrix} \mathbf{I}_3 & \mathbf{P}_i^0(1:3) \\ \mathbf{0}_3^T & 1 \end{bmatrix} \quad (7)$$

Then the position and speed of the heel are determined by:

$$\mathbf{P}_{heel}^0 = \mathbf{H}_{heel}^0(1:3,4) \quad (8)$$

$$\dot{\mathbf{P}}_{heel}^0 = \tilde{p} \cdot \tilde{f} \cdot \mathbf{P}_{heel}^0 = \begin{bmatrix} 0 & -\omega_z & \omega_y & v_1 \\ \omega_z & 0 & -\omega_x & v_2 \\ -\omega_y & \omega_x & 0 & v_3 \\ 0 & 0 & 0 & 0 \end{bmatrix} \cdot \mathbf{P}_{heel}^0 \quad (9)$$

The distance with respect to the ground is:

$$dz = \mathbf{P}_i^0[3] - \mathbf{P}_0^0[3]. \quad (10)$$

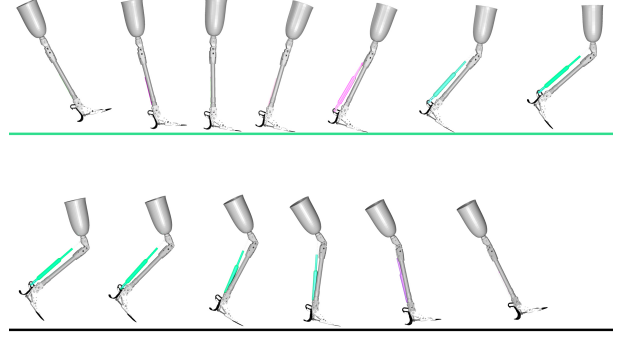


Fig. 7: Human gait overview of the simulation (green is the unloaded and purple is the loaded telescopic spring).

If there is an impact on the ground, the following normal force F_N is calculated:

$$F_N = \begin{cases} -k \cdot dz + l \cdot \dot{\mathbf{P}}_{heel}^0[3] & \text{if } \dot{\mathbf{P}}_{heel}^0[3] \geq 0 \\ -k \cdot dz & \text{if } \dot{\mathbf{P}}_{heel}^0[3] < 0 \\ 0 & \text{if } (F_N < 0) \vee (\text{no contact}) \end{cases} \quad (11)$$

The wrench at the output is:

$$W_{heel} = \begin{cases} [0; 0; 0; \mu \cdot \dot{\mathbf{P}}_{heel}^0 \cdot dz; 0; F_N] & \text{if hit heel} \\ \mathbf{0}_6^T & \text{if not hit heel} \end{cases} \quad (12)$$

where μ is the friction coefficient of the ground. Then the final wrench at the interaction point is $(Ad_{H_{ip}^{-1}})^T \cdot W_{heel}$.

F. Model Overview

The inputs of the model are the torque applied by the amputee at the hip joint of the residual limb and the forces from the sound leg. In order to validate the dynamics of the model, the hip angles of the amputee measured during the tests are used. The hip angle is tracked by a PD-controller to derive the torque of the hip joint. Furthermore, the force of the sound leg is put in the model by applying the ground reaction forces of the sound leg on the x and z direction to the hip. Fig. 7 shows an example of gait pattern for normal walking in a simulation of the dynamic model.

IV. VALIDATION OF THE MODEL

In this Section, we validate the dynamic model by using real inputs as taken from experimental tests done with a unilateral transfemoral amputee participant.

A. Experimental Test Set-up

In this study the participant was asked to perform an even ground walking on the R-mill, the 3D rehabilitation tread-mill instrumented with force sensors (Forcelink B.V., The Netherlands), at normal speed (4.6 km/h) by using the WalkMECH. The kinematic data are measured with a PTI VisualeyzeTM motion capture system (PTI, Canada) for defining:

- Prosthetic and intact limbs' joint kinematics;



Fig. 8: The participant is wearing the prosthesis with his own socket.

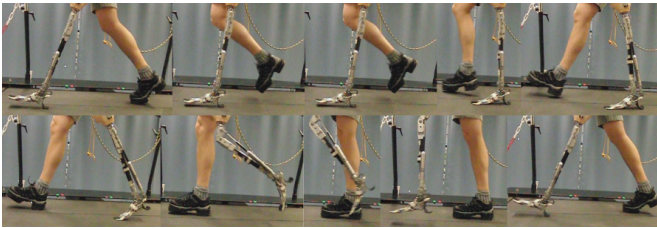


Fig. 9: Gait cycle of the amputee subject.

- Hip joint and center of total body (assumed at chest cavity) kinematics in Cartesian coordinates (x,y,z) with respect to the reference coordinate frame on the ground.

The kinetic data are measured from the R-mill for defining the ground reaction forces from both prosthetic and intact limbs. Together with the kinetic and kinematics data, an analysis of the biomechanical power flow (energy absorption and generation) of the ankle, knee and hip joints during the complete stride is performed with the dynamic model.

Fig. 8 shows the participant with the WalkMECH. A full gait pattern during normal walking is shown in Fig. 9.

B. Evaluation of the Model

In Fig. 10 the angles of the hip, knee and ankle are shown as derived from the simulation of the model (continuous line), Winter data [11] (dot-dashed line), measured data from the amputee subject (dashed line). From the plots, it can be seen that the angles derived from the simulation of the model are matching with the angles of the measured data from the functional tests with some small exceptions.

The ankle angle in the model simulation deviates from the measured angle just after push-off. This is due to the fact that, after push-off, the slider slides to the front position. However, if the telescope spring starts pushing before the slider is in

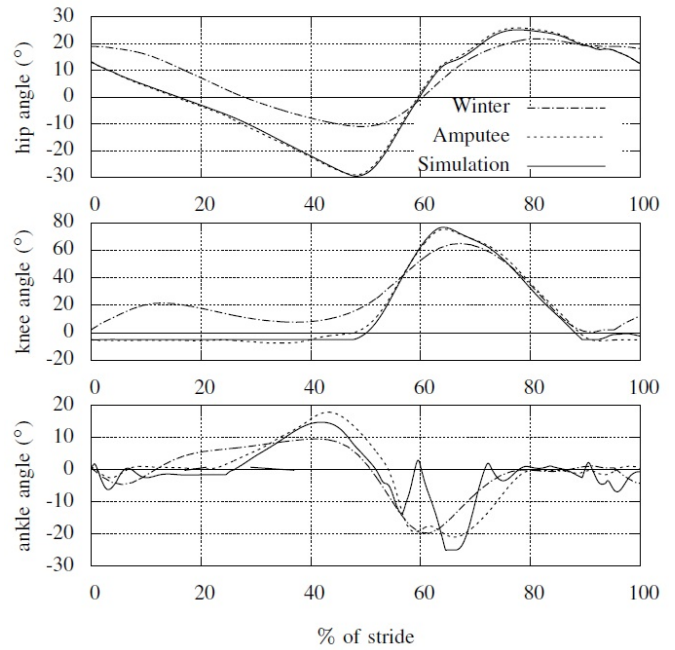


Fig. 10: Hip, knee and ankle angles comparison with real measurements (dashed line), Winter data [11] (dot-dashed line), and simulation of the model (continuous line) during normal walking

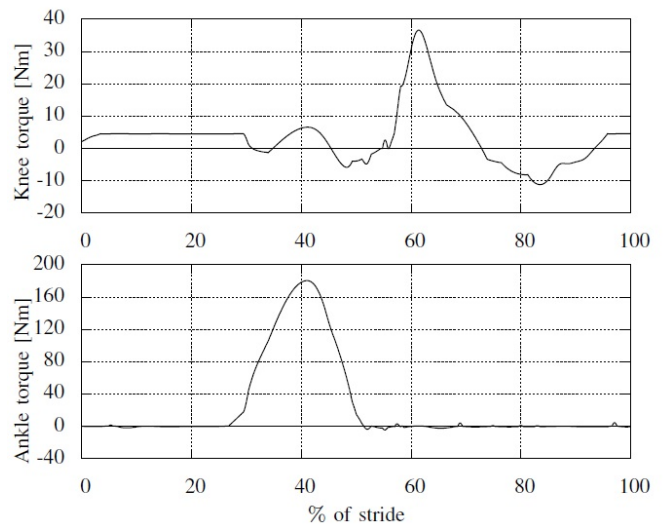


Fig. 11: The torque values around the knee and ankle joints from the model.

front position, the ankle angle is forced to move in positive direction. Then when the slider is in the front position and it is still pushing, the ankle angle is forced to move in negative direction. If the knee angle then decreases, the telescope starts pulling and the ankle is forced again to move in positive direction. This process is sensitive to gait timing and, due to small timing differences between the simulation and the real test, the model simulation and the experimental tests differ.

The joint torques of the knee and ankle are shown in Fig. 11. The positive knee torque during stance is due to the hyperextension, which is for keeping the knee joint straight

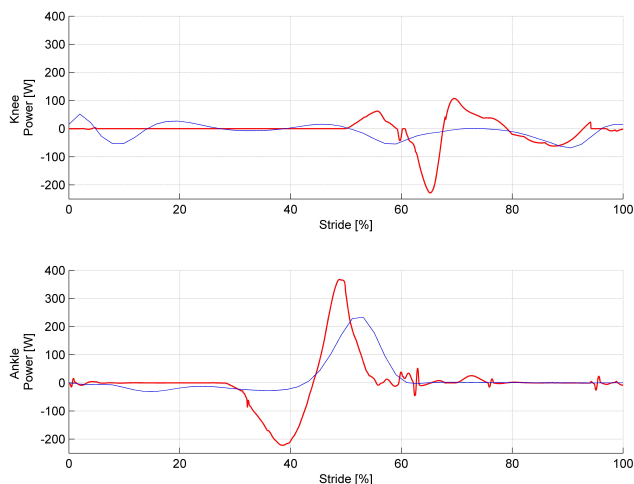


Fig. 12: The power flow of the knee and ankle joints comparison with healthy subjects (blue line) [11] and WalkMECH (red line).

during stance phase. Around 60% of stride, a positive knee torque is present due to the telescope spring that is pushing and, therefore, causing a higher hip angle input. In the ankle torque, the roll-over torque starts later in the gait because the ankle springs are only active from 0° of the ankle joint.

The power flow around the knee and ankle joints are shown in Fig. 12. In this figure, the absorption and the generation of the energy around the knee and ankle joints is shown during natural walking of healthy (blue) and amputee (red) subject walking with WalkMECH. Even though the power flow behavior is deviating from the natural one, the significant amount of ankle push-off generation has been realized, which proves the principle of the design. The power flow at the knee joint is deviating during stance since the knee is kept straight (in hyper-extension). So no power exchange takes place. During push-off there is a small positive power, which bends the knee, and after push-off the knee is slowed down by the coupling element, which results in negative power. This power is then used to swing the lower leg forward again. This extra power input causes the early absorption phase and the knee reaches hyperextension early. This faster swing is also caused by the participant with an extra hip input since he needs to be sure that the prosthesis reaches hyperextension before the heel-strike. This deviation might become less when the subject is walking on the prosthesis for a longer period. In the ankle, it is visible that the roll-over energy is stored in a smaller range because the ankle springs only start loading from 0°. Higher peak power around the ankle joint took place since almost the same amount of the energy is released in a shorter time range. This deviation occurs due to the design of the ankle joint which can be reduced by improving the design.

V. CONCLUSIONS

In this work, the dynamic model of the transfemoral prosthesis prototype, WalkMECH has been built as described

with screw theory and it has been validated through the experimental tests. The model can be used to produce the torque and power plots, which can show the performance of the prosthesis and therefore can be used to improve the mechanical design of the prototype. The torque and power plots are used to create more insight in the energetic behaviour of the prosthesis. These torque and power plots show similar behavior with the healthy human torque and power profiles with deviations that needs to be improved.

ACKNOWLEDGMENTS

The authors would like to thank the participant for the volunteering the functional tests of the prototype. This work has been funded by the Dutch Technology Foundation STW as part of the project REFLEX-LEG under the grant no. 08003.

REFERENCES

- [1] S.M. Behrens, R. Unal, E.E.G. Hekman, R. Carloni, S. Stramigioli, and H.F.J.M. Koopman, "Design of a Fully-Passive Transfemoral Prosthesis Prototype", *IEEE/EMBS International Conference on Engineering in Medicine and Biology Society*, 2011.
- [2] R. Unal, R. Carloni, S.M. Behrens, E.E.G. Hekman, S. Stramigioli, and H.F.J.M. Koopman, "Towards a fully passive transfemoral prosthesis for normal walking", *IEEE/RAS-EMBS International Conference on Biomedical Robotics and Biomechanics*, 2012.
- [3] R. Unal, R. Carloni, E.E.G. Hekman, S. Stramigioli, and H.F.J.M. Koopman, "Conceptual Design of an Energy Efficient Transfemoral Prosthesis", *IEEE/RSJ International Conference on Intelligent Robots and Systems*, 2010.
- [4] R. Unal, S.M. Behrens, R. Carloni, E.E.G. Hekman, S. Stramigioli, and H.F.J.M. Koopman, "Prototype design and realization of an innovative energy efficient transfemoral prosthesis", *IEEE/RAS-EMBS International Conference on Biomedical Robotics and Biomechanics*, 2010.
- [5] M. Stelzer and O. von Stryk, "Efficient forward dynamics simulation and optimization of human body dynamics", *ZAMM-Journal of Applied Mathematics and Mechanics/Zeitschrift für Angewandte Mathematik und Mechanik*, vol. 86, no. 10, pp. 828–840, 2006.
- [6] V. Berbyuk, G. Grasyuk, and N. Nishchenko, "Mathematical modeling of the dynamics of the human gait in the saggital plane", *Journal of Mathematical Sciences*, vol. 96, no. 2, pp. 3047–3056, 1999.
- [7] V. Berbyuk and B. Lytvyn, "Mathematical modeling of human walking on the basis of optimization of controlled processes in biodynamical systems", *Journal of Mathematical Sciences*, vol. 104, no. 5, pp. 1575–1586, 2001.
- [8] F.E. Zajac, R.R. Neptune, and S.A. Kautz, "Biomechanics and muscle coordination of human walking Part I: Introduction to concepts, power transfer, dynamics and simulations", *Gait and Posture*, vol 16, pp. 215–232, 2002.
- [9] F.E. Zajac, R.R. Neptune, and S.A. Kautz, "Biomechanics and muscle coordination of human walking Part II: Lessons from dynamical simulations and clinical implications", *Gait and Posture*, vol 17, pp. 1–17, 2003.
- [10] S. Pejhan, F. Farahmand, and M. Parnianpour, "Design Optimization of an Above-Knee Prosthesis Based on the Kinematics of Gait", *IEEE/EMBS International Conference on Engineering in Medicine and Biology Society*, 2008.
- [11] D.A. Winter, *The Biomechanics and Motor Control of Human Gait: Normal, Elderly, and Pathological*, University of Waterloo Press, 1991.
- [12] V. Duindam, A. Macchelli, S. Stramigioli, and H. Bruyninckx, "Modeling and Control of Complex Physical Systems - The Port-Hamiltonian Approach". Springer, 2009.
- [13] V. Duindam and S. Stramigioli, *Modeling and control for efficient bipedal walking robots: A port-based approach*, Springer Tracts in Advanced Robotics, Vol. 53, Springer, 2009.